Benjamin J. Zimmer
Meikle Automation,
Kitchener, Ontario, Canada

Stanley P. Lipshitz

Kirsten A. Morris

Department of Applied Mathematics,
University of Waterloo,
Waterloo, Ontario, Canada

John Vanderkooy
Department of Physics,
University of Waterloo,
Waterloo, Ontario, Canada

Edmund E. Obasi
RDWI Ltd.,
Calgary, Alberta, Canada

An Improved Acoustic Model for Active Noise Control in a Duct

This paper presents a model of sound propagation in a duct, for the purpose of active noise control. A physical model generally different from those explored in much of the literature is derived, with non-constant acoustic load impedance at the one end, and a coupled disturbance loudspeaker model at the other end. Experimental results are presented which validate the derived transfer function. [DOI: 10.1115/1.1592192]

1 Introduction

Various control techniques have been applied to the problem of active noise control including feedback and feedforward algorithms, utilizing both adaptive and robust designs [1]. Inherent in most control methodologies is the need to model the system to be controlled. The sensor(s), actuator(s), and the acoustic behavior of the path between the disturbance and location of noise control all need to be included. With the aid of a valid mathematical model, one can better understand system behavior in the face of changing system parameters. Also, accurate determination of system behavior allows high-performance controller designs since the potentially destabilizing path from actuator to sensor is modeled. Furthermore, an accurate model leads to computer simulations that can be used to predict experimental performance.

The physical system is shown in Fig. 1. It is a rigid duct of length L with a source loudspeaker at one end $(x=0)$ and open at the other $(x=L)$, herein called the *disturbance* and *open* ends, respectively. The duct has a circular cross section of radius a and spatial coordinate x. There is a sensor microphone located at $x=x_a$ and a canceller loudspeaker located at $x=x_c$. The parameters for the experimental apparatus used are in Table 1.

Modelling the propagation of sound in a duct is a classic problem and under common low-frequency assumptions, the sound waves propagating in a rigid tube are planar, or one dimensional in nature [[2], p. 38]. Various boundary conditions are employed in the literature.

One such approach [3] is to model both ends as perfectly open by setting the pressures equal to zero. This is an unrealizable case where no sound at all escapes from the ends of the duct and is inappropriate for application to active noise control, because the amount of sound escaping from the open end is often the quantity to be controlled. In Refs. [4–8] a mixed absorptive/reflective boundary condition is used at the open end of the duct. This leads to a nonzero constant impedance. However, the analytical solution for the open end impedance of a duct [9] demonstrates that the impedance is highly frequency dependent. Thus, the physics of sound propagation in a tube show that, although small, the pressure $p(x,t)$ is not zero at an open end and that the impedance is strongly frequency dependent. Hu [10] derives a transfer function for a duct with variable impedances at each end. No model for the impedances is given. Also, a time-domain interpretation for the model is not provided.

The boundary condition at the disturbance end of the duct is also treated in a variety of ways in the literature. The disturbance loudspeaker has been considered to be a source of pressure [4,7]. However, a loudspeaker is closer to a volume velocity source than a pressure source. The disturbance speaker cone velocity can be used as the input to the duct transfer function. This approach is explored in Refs. [11,12]. Feedback is introduced to a loudspeaker so that its response is close to that of a pure volume velocity source. This approach does not include the interaction between the loudspeaker and the duct. Even when undriven, the loudspeaker acts as a mechanical mass-spring-damper system and there is coupling between the duct and the loudspeaker. Thus, a system model which assumes a pure pressure or volume velocity source neglects this coupling. A full electromechanical model of the loudspeaker should be coupled to the duct model to properly represent the disturbance end.

In this paper, a duct model is developed. First, we cite the analytic solution to the frequency-dependent impedance of the open end of the duct [9,13]. This model is coupled to the duct system as the open end boundary condition. Next, a model of a dynamic loudspeaker is coupled to the duct system as a source end boundary condition. A classic one-dimensional model for sound propagation inside the duct will be given, and the fully coupled system will then be solved in the frequency domain. Experimental results are presented that validate the derived model of the duct system.

2 Open End Boundary Condition

The open end of the duct results in a partially reflective and partially absorptive boundary condition. If the amount of reflection is independent of frequency, the boundary condition can be written in the time domain as [8]

$$\frac{p(L,t)}{v(L,t)}=K\rho_0 c, \tag{1}$$

Contributed by the Dynamic Systems, Measurement, and Control Division of THE AMERICAN SOCIETY OF MECHANICAL ENGINEERS for publication in the ASME JOURNAL OF DYNAMIC SYSTEMS, MEASUREMENT, AND CONTROL. Manuscript received by the ASME Dynamic Systems and Control Division September 7, 2001; final revision, March 29, 2003. Associate Editor: R. Mukherjee.

where $p(x,t)$ and $v(x,t)$ represent pressure and velocity, respectively, ρ_0 is the density of the medium and c is the speed of sound in the medium. The quantity $\rho_0 c$ is the specific acoustic impedance for free propagation in the medium.

When $K=0$, this is equivalent to the zero-pressure model of the open end at $x=L$ where the wave is totally reflected but inverted, and when $K=\infty$, this is equivalent to a closed end at $x=L$ where the wave is totally reflected without inversion. When $K=1$, the end impedance of the duct is equal to the medium's specific acoustic impedance, and as such the wave is totally transmitted, analogous to a semi-infinite duct.

Let $\hat{p}(L,s)$ indicate the Laplace transform of $p(L,t)$, and define $\hat{v}(L,s)$ similarly. The specific acoustic impedance of the open end of the duct is

$$Z_L(s)=\frac{\hat{p}(L,s)}{\hat{v}(L,s)}. \tag{2}$$

The impedance Z_L is a quantitative measure of the manner in which the air outside the duct reacts against the sound waves in the duct. If $K\neq 0$ or ∞, energy is radiated by the duct into the air. Part of this radiated energy is real and propagates into the far-field and the remainder is stored or reactive energy. The amount of energy radiated results from the real part of Z_L and the reactive energy results from the imaginary part of Z_L. The open end boundary condition (1) in the frequency domain is

$$\hat{p}(L,s)=Z_L\hat{v}(L,s), \tag{3}$$

where

$$Z_L(s)=\rho_0 c\,\frac{1+R}{1-R} \tag{4}$$

is the **specific acoustic impedance** of the end, and R is the reflection coefficient of the end of the duct. Let J_1, N_1, I_1, K_1 indicate Bessel functions, a the radius of the duct, $k=2\pi f/c$ where f is the radiation frequency and c is the wave propagation speed. From Refs. [9] and [[13], p. 1529], the analytical solution for R is

$$R=-|R|e^{2ikl},$$

where the end correction l and magnitude $|R|$ are defined as follows:

$$l=\frac{a}{\pi}\int_0^{ka}\frac{\log\{\pi J_1(x)[(J_1(x))^2+(N_1(x))^2]^{1/2}\}}{x[(ka)^2-x^2]^{1/2}}dx$$

$$+\frac{1}{\pi}\int_0^{\infty}\frac{\log[1/(2I_1(x)K_1(x))]}{x[x^2+(ka)^2]^{1/2}}dx,$$

$$|R|=\exp\left\{-\frac{2ka}{\pi}\int_0^{ka}\frac{\tan^{-1}(J_1(x)/N_1(x))}{x[(ka)^2-x^2]^{1/2}}dx\right\}.$$

Figure 2 shows the frequency dependent nature of the complex end impedance from Eq. (4) as well as the approximation (8) (defined below). It can be seen that the end impedance changes in nature from predominantly reactive to predominantly resistive as frequency increases. For the dimensions of our duct (Table I), the normalization parameter $2\pi a/c=0.0006\pi$ and so the normalized frequency is 1 when the actual frequency is 537 Hz. It can be seen from the plot that there is a significant variation in both the real and imaginary parts of the impedance over the frequency range 0–500 Hz.

Table 1 Parameters

L	duct length	3.54 m
a	duct radius	.101m
ρ	density of air	1.20 km/m^3
c	speed of sound in air	341 m/s
R_2	end impedance parameter	$\rho_0 c/\pi a^2$ mks ac.Ω
R_1	end impedance parameter	$0.504R_2$ mks ac.Ω
C	end impedance parameter	$5.44a^3/\rho_0 c^2$ m^5/N
M	end impedance parameter	$0.1952\rho_0/a$ kg/m^4
m_D	disturbance speaker's cone effective mass	.015 kg
k_D	disturbance speaker's cone suspension stiffness	810.87 N/m
R_{coil}	electrical resistance of voice coil (disturbance)	6.0 Ω
Bl	$B\cdot l$ magnetic voice coil motor (disturbance)	5.6 N/A
r_d	disturbance speaker's effective radius	.087 m
m_c	canceller speaker effective mass	.006394 kg
k_c	canceller speaker stiffness parameter	673.7 N/m
R_c	electrical resistance of voice coil (canceller)	6.05 Ω
Bl_c	$B\cdot l$ magnetic voice coil motor (canceller)	5.68 N/A
r_c	canceller speaker's effective radius	.06 m
x_a	mid-microphone location	1.095 m
x_c	canceller speaker location	2.32 m

The specific acoustic impedance of the duct at $x=L$, $Z_L(s)$, given in Eq. (4), is approximated by a rational function in Ref. [[14] pg. 122] using an electrical circuit analogy. The differential equations that model this impedance are as follows. Here $P(t)$ is the driving voltage, $P_c(t)$ is capacitor voltage, and $V_m(t)$ is the inductor current. (Note that $P(t)$ and $V(t)$ are equivalent to the acoustic pressure $p(L,t)$ and velocity $v(L,t)$ respectively.)

$$\frac{dP_c}{dt}=P_c\left(-\frac{1}{C}\right)\left(\frac{1}{R_1}+\frac{1}{R_2}\right)-\frac{1}{CR_2}P, \tag{5}$$

$$\frac{dV_m}{dt}=\frac{P(t)}{M}, \tag{6}$$

$$V(t)=\frac{1}{R_2}P(t)+\frac{1}{R_2}P_c(t)+V_m(t). \tag{7}$$

The corresponding impedance $\hat{P}(L,s)/\hat{V}(s)$ of this model is

$$Z_L(s)=\pi a^2\frac{(R_1+R_2)Ms+R_1R_2MCs^2}{(R_1+R_2)+(M+R_1R_2C)s+R_1MCs^2}. \tag{8}$$

The parameter values are as given in Ref. [14], and are in Table 1.

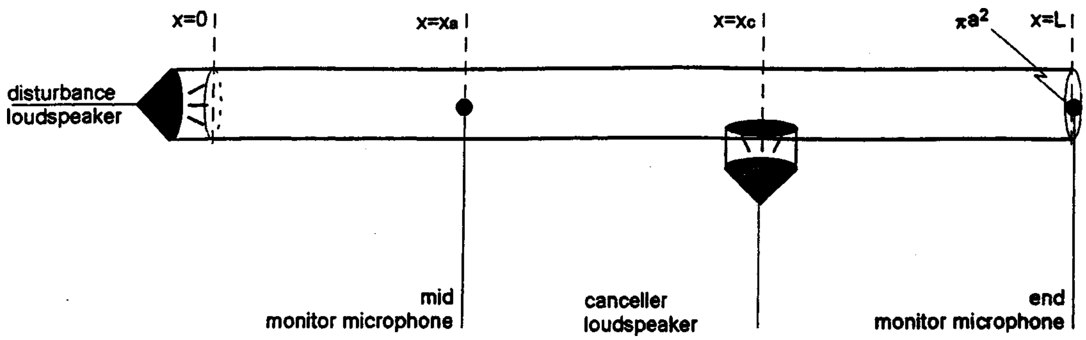

Fig. 1 Acoustical duct system.

The impedance of this rational approximation closely matches the original impedance (see Fig. 2). The impedance (8) will henceforth be used as the impedance for the open end.

3 Disturbance End Boundary Condition

A loudspeaker is mounted at the disturbance end of the duct, acting as a source of noise. It is a common approach in the literature to impose the boundary condition of a closed end here. In this case, the loudspeaker is considered to be a volume velocity source, injecting a signal $V_D(t)$, and the particle velocity in the duct at the disturbance end is

$$v(0,t)=\frac{V_D(t)}{\pi a^2}, \tag{9}$$

where πa^2 is the cross-sectional area of the duct.

This condition implies that, when undriven, the loudspeaker acts as a perfectly rigid end, with zero velocity. In fact, a loudspeaker connected to an amplifier has compliance, mass and damping even when undriven, and thus will not act as a perfectly rigid end.

A loudspeaker diaphragm moves when voltage across the input terminals causes current flow in the voice coil. The voice coil is in the magnetic field of the permanent magnet and the current produces a driving force which moves the attached diaphragm, generating an acoustic pressure. Compliance, mass, and damping exist in the loudspeaker from the spider and surround which attach the diaphragm to the frame. The movement of the voice coil within the permanent magnetic field induces a voltage, called the back EMF. The back EMF tends to oppose the driving voltage, and is proportional to the diaphragm velocity. The loudspeaker operates as a piston at low frequencies and can be modeled as a

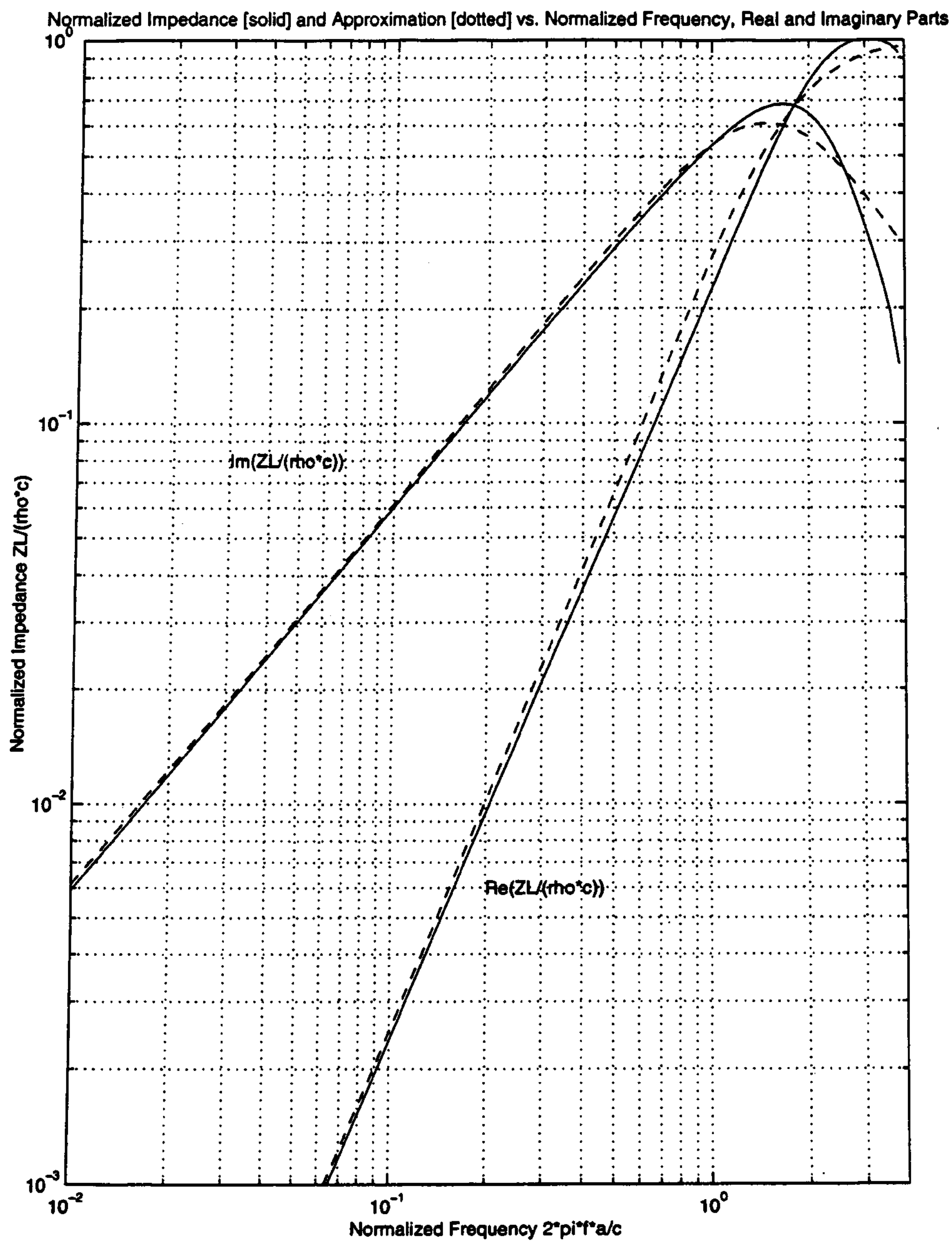

Fig. 2 Normalized impedance $Z_L/\rho_0 c$ (Solid) and the rational approximation to $Z_L/\rho_0 c$(*dashed*). (For our duct, normalized frequency is $f/537$.)

simple mass-spring-damper system where the mass is that of the diaphragm and voice coil and the stiffness is due to the spider and surround. The effective cone mass m_D typically includes a contribution due to the reactive component of the air load on the front and back of the loudspeaker diaphragm. We shall account for this discrepancy by using a effective value for m_D different from the free-air value.

The governing equations of the loudspeaker are [[14], e.g.]

$$F_{motor}=(Bl)i, \tag{10}$$

$$V_{back}=(Bl)\dot{x}_D, \tag{11}$$

$$i=\frac{E_D-V_{back}}{R_{coil}}, \tag{12}$$

$$F=m_D\ddot{x}_D+k_Dx_D+A_DP_D. \tag{13}$$

The loudspeaker suspension mechanical damping has been neglected in this model because it is dominated by the electrical damping due to V_{back}. Solving, we obtain

$$m_D\ddot{x}_D(t)+d_D\dot{x}_D(t)+k_Dx_D(t)=g(t)-A_DP_D(t), \tag{14}$$

where $d_D=[(Bl)^2/R_{coil}]$, $A_D=\pi r_D^2$, and $g(t)=(Bl/R_{coil})E_D(t)$ is the driving force of the loudspeaker.

The loudspeaker is coupled to the duct by

$$A_D\dot{x}_D(t)=\pi a^2 v(0,t) \tag{15}$$

and

$$P_D(t)=p(0,t), \tag{16}$$

where $v(x,t)$ is the particle velocity in the duct and $p(x,t)$ is the pressure in the duct.

Taking Laplace transforms of the loudspeaker model in Eq. (14), we obtain

$$A_D\hat{p}(0,s)=\frac{Bl}{R_{coil}}\hat{E}_D(s)-Z_0(s)\hat{v}(0,s), \tag{17}$$

where

$$Z_0(s)=\frac{\pi a^2}{A_Ds}(m_Ds^2+d_Ds+k_D)$$

is the mechanical impedance of the loudspeaker, and $\hat{E}_D(s)$ is the Laplace transform of the driving voltage $E_D(t)$.

Note that when the loudspeaker is undriven ($\hat{E}_D(s)=0$), the particle velocity at $x=0$, $\hat{v}(0,s)$, is not necessarily zero. It is dependent on Z_0, the impedance of the loudspeaker, and $\hat{p}(0,s)$. The electrodynamic braking of the loudspeaker cone by its driving amplifier's zero output impedance is modeled by this equation.

4 Duct Model

The duct is considered to be a finite-length, hard-walled structure, with sound dissipation only at the ends. The pressure in the duct is a function of space and time $p(x,t)$, particle velocity is $v(x,t)$, and air density is $\rho(x,t)$.

The following well-known equations describe the propagation of sound in a one-dimensional duct, e.g., Ref. [15]. Here $V(x,t)$ is a volume velocity source per unit length of the duct due to the canceller loudspeaker,

$$\frac{1}{c^2}\frac{\partial p}{\partial t}=-\frac{\partial v}{\partial x}\rho_0+\frac{1}{\pi a^2}\rho_0 V(x,t), \tag{18}$$

$$\rho_0\frac{\partial}{\partial t}v(x,t)=-\frac{\partial}{\partial x}p(x,t). \tag{19}$$

The one-dimensional model used here assumes that the only propagating waves are the axial plane waves. The transverse waves attenuate rapidly and are neglected. For a circular duct of radius a, this assumption is valid for frequencies below the cutoff frequency of $0.293c/a$ [[16], Sec. 9.2]. For our system, $a=0.101m$ and $c=341$ m/s, leading to a cutoff frequency of about 989 Hz. Thus, at frequencies below 900 Hz this one-dimensional model is valid.

Let $V_c(t)$ represent the total volume velocity (in m^3/s) of the canceller loudspeaker, distributed over a length $2r_c$ of the duct at location $x=x_c$. The volume velocity $V(x,t)$ per unit length is

$$V(x,t)=\begin{cases}0, & x<x_c-r_c\\ V_c(t)\dfrac{2}{\pi r_c^2}\sqrt{r_c^2-(x-x_c)^2}, & x_c-r_c\leq x\leq x_c+r_c.\\ 0, & x_c+r_c<x\end{cases} \tag{20}$$

The volume velocity is related to the voltage $E_c(t)$ applied to the loudspeaker by a model identical to that described above for the disturbance loudspeaker

$$\hat{V}_c(s)=\frac{Bl_c}{R_cZ_c(s)}\hat{E}_c(s), \tag{21}$$

where

$$Z_c(s)=\frac{m_cs^2+d_cs+k_c}{\pi r_c^2 s}.$$

Equations (18) and (19) with the model for the open end at $x=L$ (Eqs. (5–7)) and the loudspeaker model at $x=0$ (Eqs. (14–16)) form a boundary value problem that fully describes the sound dynamics in the duct. Regarding $V_c(t)$ and $E_D(t)$ as external inputs, with state $(p(x,t),v(x,t),P_c(t),V_m(t),x_D(t),\dot{x}_D(t))$, this boundary value problem is mathematically well-posed with state-space $\mathcal{L}_2(0,L)\times\mathcal{L}_2(0,L)\times R^4$ (Appendix A). This implies that the controlled system with inputs E_c and E_D is well-posed.

We now derive the transfer function. This will be used to verify the model by comparing the theoretical and experimental frequency responses. Assume that the duct is initially in a state of rest. Taking Laplace transforms with respect to time of Eqs. (18) and (19), and writing $\hat{p}(x,s)=\mathcal{L}\{p(x,t)\}$, etc., we obtain

$$\left.\begin{aligned}\hat{p}_{xx}(x)-\left(\frac{s}{c}\right)^2\hat{p}(x)&=f(x)\\ \hat{p}_x(L)&=\frac{-\rho_0 s}{Z_L(s)}\hat{p}(L)\\ \hat{p}_x(0)&=\rho_0 s\left(\frac{A_D\hat{p}(0)-g(s)}{Z_0(s)}\right)\end{aligned}\right\}, \tag{22}$$

where $f(x)=(-\rho_0 s/\pi a^2)\hat{V}(x,s)$, $g(s)=(Bl/R_{coil})\hat{E}_D(s)$.

The set of Eqs. (22) is a linear boundary value problem for $\hat{p}$ as a function of x. This boundary value problem is solved in Appendix B, using a standard Green's-function method. Define

$$\alpha_0(s)=\frac{Z_0(s)-\rho_0cA_D}{Z_0(s)+\rho_0cA_D}\text{ and }\alpha_L(s)=\frac{Z_L(s)-\rho_0c}{Z_L(s)+\rho_0c}.$$

The transfer function that relates the pressure measured at x to the voltage applied to the disturbance loudspeaker at $x=0$ is

$$G_d(x,s)=e^{-x\,s/c}G_{do}(x,s), \tag{23}$$

where

$$G_{do}(x,s)=\frac{Bl\rho_0c(1+\alpha_0(s))}{2R_{coil}Z_0(s)(1-\alpha_0(s)\alpha_L(s)e^{-2L\,s/c})}\times(1+\alpha_L(s)e^{2(x-L)\,(s/c)}). \tag{24}$$

Define $J(z)=2J(1,z)/z$ where $J(1,z)$ indicates the Bessel function of the first kind of order 1. The transfer function that relates pressure measured at x to the voltage applied to the canceller loudspeaker at $x=x_c$ is

$$\frac{Bl\rho_0c}{2R_cZ_c(s)\pi a^2(1-\alpha_0(s)\alpha_L(s)e^{-2L\,s/c})}\tilde{G}(s),$$

where

$$\tilde{G}(s)=\begin{cases} (\alpha_L(s)e^{(-2L+x)(s/c)}+e^{-(s/c)x})\left(e^{x_c(s/c)}J\left(-ir_c\frac{s}{c}\right)+\alpha_0(s)e^{-x_c(s/c)}J\left(ir_c\frac{s}{c}\right)\right) & 0<x_c\leq x \\ \left(\alpha_L(s)e^{(x_c-2L)(s/c)}J\left(-ir_c\frac{s}{c}\right)+e^{-(s/c)x_c}J\left(ir_c\frac{s}{c}\right)\right)\left(e^{x(s/c)}+\alpha_0(s)e^{-x(s/c)}\right) & x\leq x_c<L \end{cases}. \tag{25}$$

The speaker cone radius r_c is very small, and so the terms $J(z)$ in the above function are close to the constant value 1 over the frequency range of interest, $0-500$ Hz. Approximating $J(z)$ by the constant value 1, we obtain

$$G_c(x,s)=e^{-|x-x_c|(s/c)}G_{co}(s), \tag{26}$$

where we define

$$R(s)=\frac{Bl\rho_0 c}{2R_c Z_c(s)\pi a^2(1-\alpha_0(s)\alpha_L(s)e^{-2L\,s/c})}, \tag{27}$$

$$G_{co}(s)=R(s)\begin{cases}(1+\alpha_L(s)e^{2(x-L)(s/c)})(1+\alpha_0(s)e^{-2x_c(s/c)}) & 0<x_c\leq x \\ (1+\alpha_L(s)e^{2(x_c-L)(s/c)})(1+\alpha_0(s)e^{-2x(s/c)}) & x\leq x_c<L\end{cases}. \tag{28}$$

This is the same transfer function obtained if the canceller loudspeaker is regarded as a point source of volume velocity located at $x=x_c$. The spatial distribution of this loudspeaker has a negligible effect on the system frequency response over the frequency range of interest.

5 Experimental Verification

Our experimental duct setup, shown in Fig. 1, consisted of the following components. The duct itself, of length 3.54 m, is a PVC 1120 water pipe with an 8-in. nominal inner diameter, and a wall thickness of 0.375 in. The disturbance loudspeaker is a Philips 9710/M8 8.5-in. dimeter, 8-ohm, full-range driver which fits snugly into the pipe's coupling section. The canceller loudspeaker is a Marsland "Linear B" 6.5-in., 8-ohm, high-compliance driver mounted with an adapter flange into the side of the duct at a distance of 2.32 m from the disturbance end. The reference and error microphones are Panasonic miniature WM-63 electret, pressure-responding capsules, with appropriate simple RC powering circuits. Each is mounted on a stiff wire so as to place the capsule on the center line of the duct, at the positions of the mid microphone (distance 1.095 m from the disturbance end), and end microphone (in the plane of the open end, 3.54 m from the disturbance end). The open end of the duct is well away from acoustic obstructions. A dSPACE model DS1102 DSP Controller Board was used to obtain the frequency response in conjunction with the dSPACE "Real-Time Interface" software which interfaces with MATLAB (with Simulink and the Real-Time Workshop).

From Eq. (14), the transfer function from drive voltage to cone acceleration is

$$\frac{\hat{a}_{cone}}{\hat{E}_D}=\frac{Bls^2}{R_{coil}\left(m_D s^2+\frac{(Bl)^2}{R_{coil}}s+k_D\right)}.$$

As a validation of this loudspeaker model, the disturbance loudspeaker acceleration to input voltage response was measured in free air. Figure 3 compares the measured to the theoretical frequency responses.

It can be seen that the measurement agrees well in magnitude and phase with the loudspeaker model to 400 Hz. Beyond this frequency value, the results bear no resemblance to the second order model. This can be understood by considering that the model assumes piston-mode behavior on the part of the loudspeaker. It is common for loudspeakers of this size to have breakup modes occurring in the 400–600-Hz range. Nonetheless, in the frequency range of interest to active noise control, up to roughly 400 Hz, the second-order loudspeaker model (14) is seen to be valid.

As previously discussed, it is a common practice in the literature to apply a rigid end assumption to the $x=0$ boundary condition: $Z_0=\infty$. For the purpose of experimentally validating the simplified version of the transfer function with $Z_0=\infty$, a rigid end was created by inserting a tightly-fitted wooden plug into the disturbance end of the duct, in place of the disturbance loudspeaker. Figures 4 and 5 display the frequency responses from the canceller speaker volume velocity to the midpoint pressure. In Fig. 4 the end $x=0$ is plugged to obtain a rigid end, while the data in Fig. 5 was obtained with the disturbance speaker in place, but undriven. It can be seen from the low-frequency disagreement that the rigid end boundary condition is not appropriate when a speaker is used at the end. As can be seen in Fig. 4, agreement is very good up to roughly 500 Hz, and still somewhat valid up to 700 Hz. This illustrates the increased accuracy in the model obtained by using the frequency-dependent impedance Z_L at the open end.

Figures 6–9 illustrate the four measured voltage to pressure transfer functions, compared to the theoretical transfer function derived in Secs. 2–4. In all four figures, it can be seen that the model agrees very well with the data in the region where the loudspeaker model is valid, 50–500 Hz. Agreement is quite good up to about 900 Hz.

Figures 6 and 8 illustrate that the pressure at the $x=L$ end is quite significant, particularly at the natural frequencies of the duct. This illustrates the error of earlier models which assumed that pressure is 0 at $x=L$.

6 Conclusions

An improved analytical duct model has been experimentally verified. The necessity of carefully modeling the boundary conditions of the duct has been demonstrated.

A theoretical and fully analytical solution to the open-end impedance of the duct has been cited. An approximation of this frequency-dependent impedance was coupled to the duct system, and experimentally validated.

A loudspeaker model was coupled to the duct system model at the disturbance end, providing a better fit to experimental data than more simple boundary conditions. A loudspeaker model for the canceller signal was also included. Although this speaker has a nonconstant frequency response, the spatial distribution of the speaker was found to be insignificant over the frequency range of interest, 0–500 Hz.

The theoretical model is very accurate up to about 500 Hz, and reasonable up to the frequency where the one-dimensional assumption breaks down, about 900 Hz.

Since the model is physics based, and the parameters are carried through the model development, application of this model to other experimental configurations should be straightforward. The results obtained here for the one- dimensional duct can also be extended to analyze the three-dimensional problem, permitting the study of active noise control for more complicated applications.

Active noise control implementations could exploit the modeled transfer function. Good experimental agreement over the frequency range 0–500 Hz permits the robust design of controllers with good performance. The model can be used in computer-based controller design. In addition, accurate modeling of the feedback path from canceller loudspeaker to monitor microphone would aid the implementation of adaptive control strategies.

Appendix A: State-Space Formulation

We will now show that the duct model is mathematically well posed. Define the state $z \in \mathcal{H}$ where

$$\mathcal{H} = \mathcal{L}_2(0,L) \times \mathcal{L}_2(0,L) \times R \times R \times R \times R.$$

The Hilbert space $\mathcal{H}$ has inner product

$$\langle z,w\rangle_{\mathcal{H}} = \frac{1}{c^2\rho_o}\int_0^L z_1\overline{w_1}dx + \rho_o\int_0^L z_2\overline{w_2}dx + Cz_3\overline{w_3} + Mz_4\overline{w_4} + \frac{k_D}{\pi a^2}z_5\overline{w_5} + \frac{m_D}{\pi a^2}z_6\overline{w_6}.$$

Let Γ_L indicate function evaluation at $x=L$, Γ_0 function evaluation at $x=0$. Define the operator A on $\mathcal{H}$

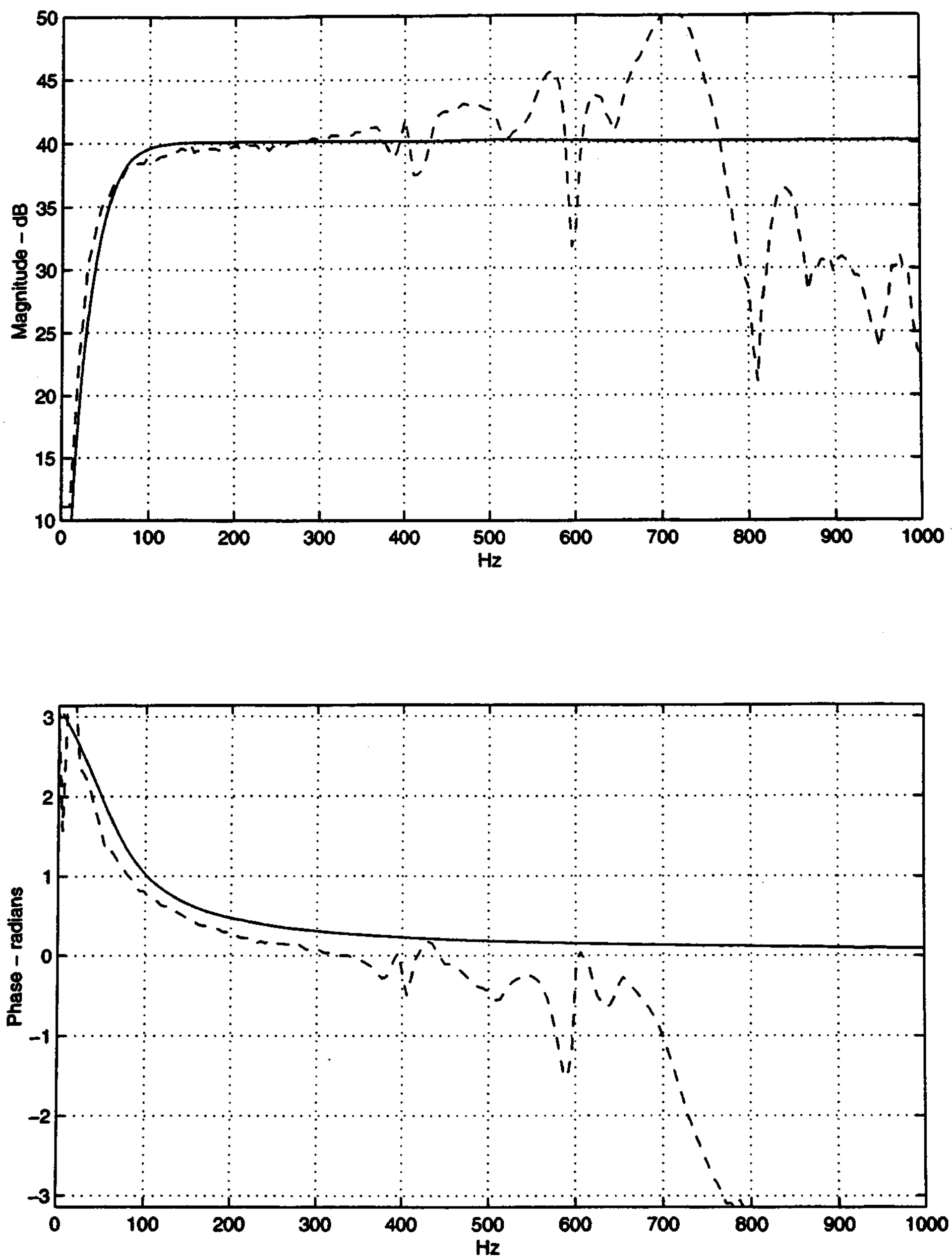

Fig. 3 Measured (dashed) and calculated (solid) input voltage to loudspeaker cone acceleration frequency responses.

$$A=\begin{bmatrix} 0 & -\rho_o c^2\frac{\partial}{\partial x} & 0 & 0 & 0 & 0 \\ -\frac{1}{\rho_o}\frac{\partial}{\partial x} & 0 & 0 & 0 & 0 & 0 \\ -\frac{1}{CR_2}\Gamma_L & 0 & -\frac{1}{C}\left(\frac{1}{R_1}+\frac{1}{R_2}\right) & 0 & 0 & 0 \\ \frac{1}{M}\Gamma_L & 0 & 0 & 0 & 0 & 0 \\ 0 & 0 & 0 & 0 & 0 & 1 \\ -\frac{A_D}{m_D}\Gamma_0 & 0 & 0 & 0 & -\frac{k_D}{m_D} & -\frac{d_D}{m_D} \end{bmatrix}$$

with domain

$$D(A)=\left\{z_1\in H^1(0,L), z_2\in H^1(0,L), z_2(L) = \frac{1}{R_2}z_1(L)+\frac{1}{R_2}z_3+z_4, z_2(0)=\frac{A_D}{\pi a^2}z_6\right\}.$$

To simplify the development of the state-space formulation, the canceller speaker volume velocity $V_c(t)$ and the disturbance speaker voltage $E_D(t)$ are set to zero. The partial differential equations for the duct noise (18)–(19), the loudspeaker equations (14)–(16) and Eqs. (5)–(7) describing the behavior at the open end can be written as $z(t)\in D(A)$ with

$$\frac{dz}{dt}=Az(t),$$

where the state $z(t)\in\mathcal{H}$ is

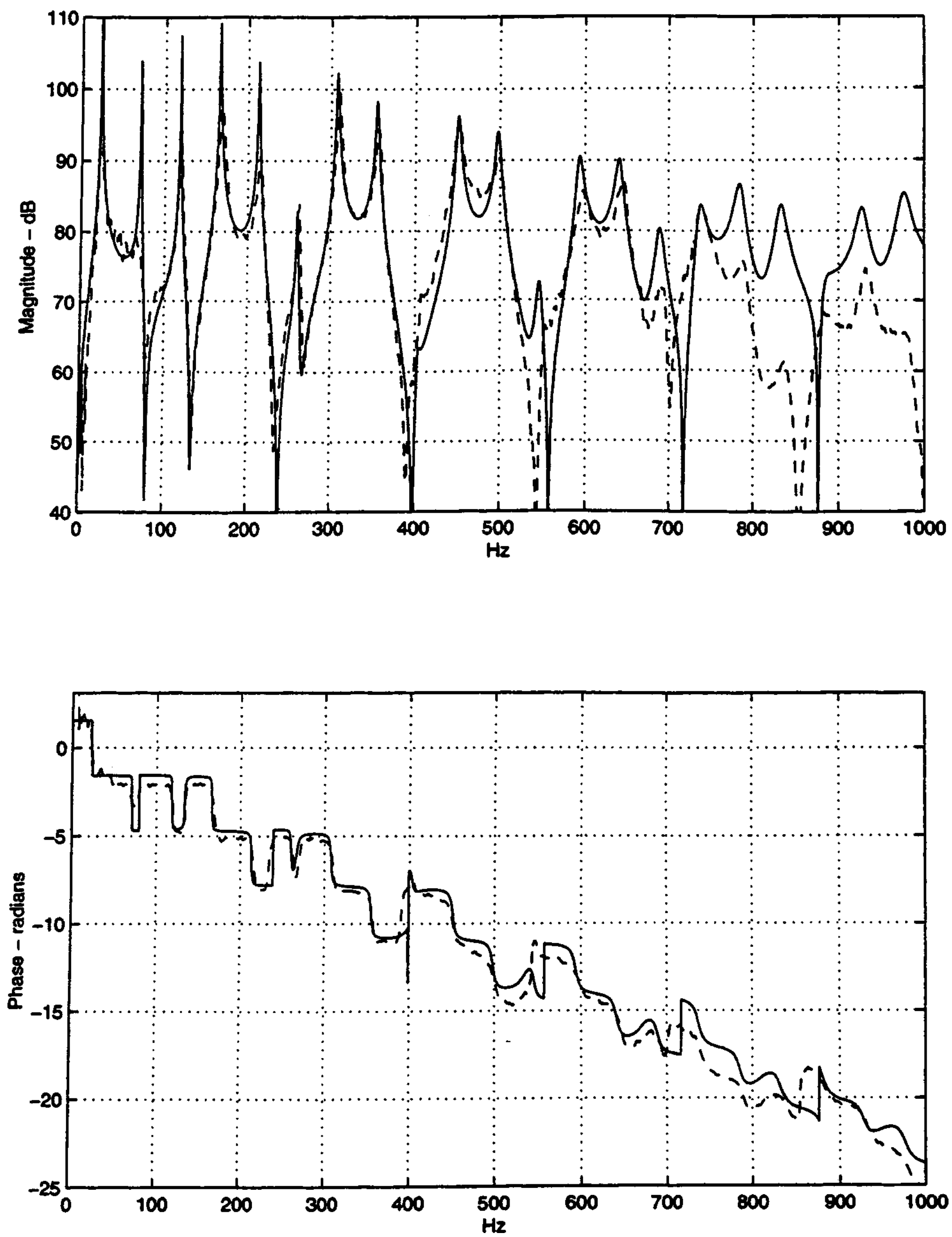

Fig. 4 Measured (dashed) and calculated (solid) canceller speaker to mid microphone frequency responses, with rigid plug at $x=0$.

$$z(t)=\begin{bmatrix} p(x,t) \\ v(x,t) \\ P_c(t) \\ P_m(t) \\ x_D(t) \\ \dot{x}_D(t) \end{bmatrix}.$$

We will use the Lumer-Phillips Theorem (e.g., Ref. [17]) to show that A generates a strongly continuous semigroup e^{At} on $\mathcal{H}$. Thus, for every initial condition $z(0)\in\mathcal{H}$ there is a unique solution to the system of differential equations that depends continuously (in the $\mathcal{H}$ norm) on $z(0)$. This will also show that the semigroup is dissipative and so if there is no disturbance voltage or canceller speaker volume velocity, then

$$\|z(t)\|_{\mathcal{H}}\leqslant\|z(0)\|_{\mathcal{H}}, \quad t\geqslant 0.$$

This will be done by showing that

(1) $\mathrm{Re}\langle Az,z\rangle_{\mathcal{H}}\leqslant 0$ for $z\in D(A)$,
(2) Range $(\lambda I-A)=\mathcal{H}$ for some λ.

(1) We will first show that $\mathrm{Re}\langle Az,z\rangle_{\mathcal{H}}\leqslant 0$, for any $z\in D(A)$,

$$\begin{aligned}\langle Az,z\rangle_{\mathcal{H}}=&-\int_0^L z_2'\overline{z_1}dx-\int_0^L z_1'\overline{z_2}dx-\frac{1}{R_2}z_1(L)\overline{z_3}\\&-\left(\frac{1}{R_1}+\frac{1}{R_2}\right)|z_3|^2+z_1(L)\overline{z_4}+\frac{k_D}{\pi a^2}z_6\overline{z_5}\\&-\frac{A_D}{\pi a^2}z_1(0)\overline{z_6}-\frac{k_D}{\pi a^2}z_5\overline{z_6}-\frac{d_D}{\pi a^2}|z_6|^2.\end{aligned}$$

Integrating the first integral by parts,

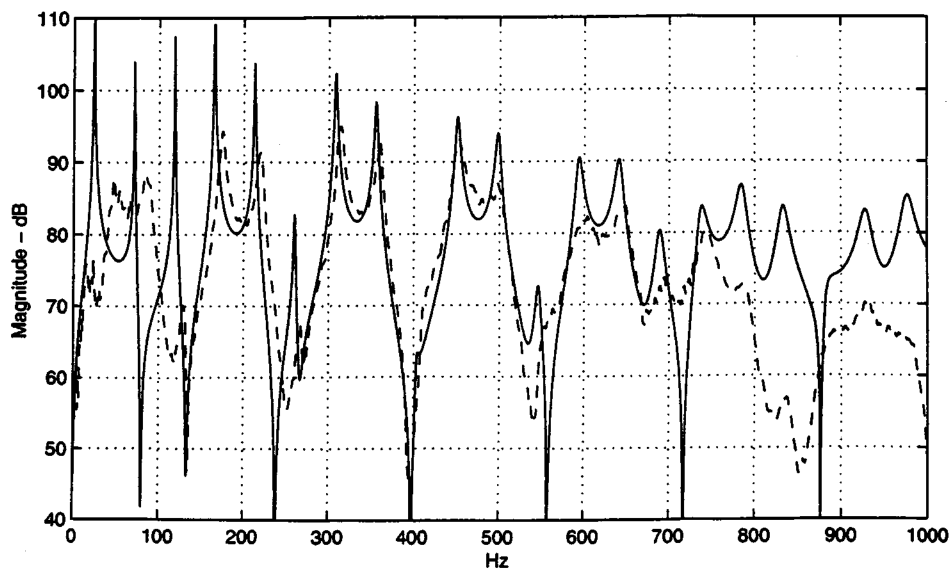

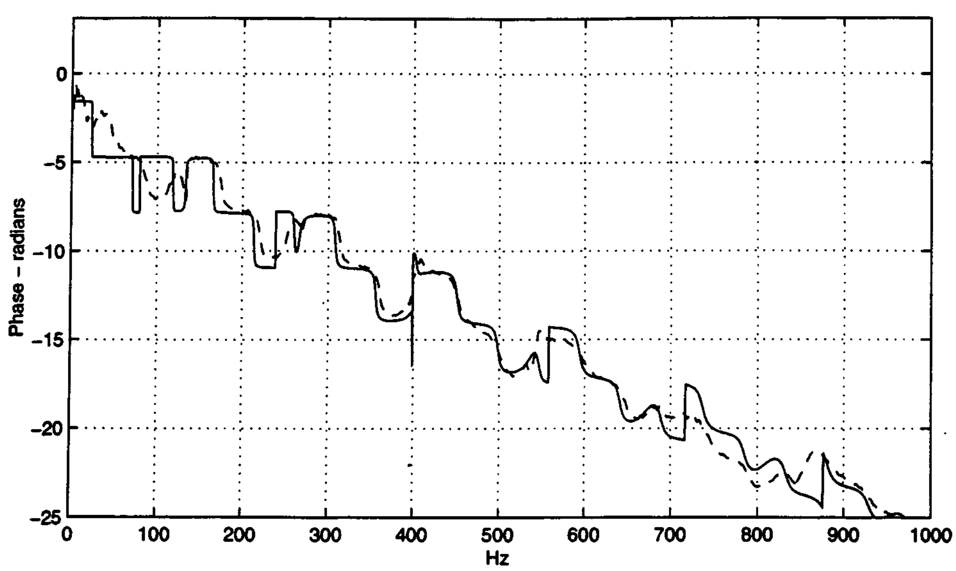

Fig. 5 Measured (dashed) canceller speaker to mid microphone frequency response, with loudspeaker at $x=0$. Calculation is with rigid.

$$\mathrm{Re}\langle Az,z\rangle_{\mathcal{H}}=\mathrm{Re}\bigg\{-z_2(L)\overline{z_1(L)}+z_2(0)\overline{z_1(0)} -\frac{1}{R_2}z_1(L)\overline{z_3}-\left(\frac{1}{R_1}+\frac{1}{R_2}\right)|z_3|^2+z_1(L)\overline{z_4} -\frac{A_D}{\pi a^2}z_1(0)\overline{z_6}-\frac{d_D}{\pi a^2}|z_6|^2\bigg\}.$$

Now apply the boundary conditions in $D(A)$:

$$\mathrm{Re}\langle Az,z\rangle_{\mathcal{H}}=\mathrm{Re}\bigg\{-\frac{1}{R_2}|z_1(L)|^2-\frac{1}{R_2}z_3\overline{z_1}(L)-z_4\overline{z_1}(L) +\frac{A_D}{\pi a^2}z_6\overline{z_1}(0)-\frac{1}{R_2}z_1(L)\overline{z_3}-\left(\frac{1}{R_1}+\frac{1}{R_2}\right)|z_3|^2 +z_1(L)\overline{z_4}-\frac{A_D}{\pi a^2}z_1(0)\overline{z_6}-\frac{d_D}{\pi a^2}|z_6|^2 \bigg\}$$

$$=\mathrm{Re}\bigg\{-\frac{1}{R_2}|z_1(L)+z_3|^2-\frac{1}{R_1}|z_3|^2 -\frac{d_D}{\pi a^2}|z_6|^2\bigg\}.$$

Thus,

$$\mathrm{Re}\langle Az,z\rangle_{\mathcal{H}}\leqslant 0$$

for all $z\in D(A)$.

(2) We now show that Range $(-A)=\mathcal{H}$. Let $y=(\phi,\psi,y_1,y_2,y_3,y_4)$ be any element of $\mathcal{H}$. We need to find $z\in D(A)$ so that

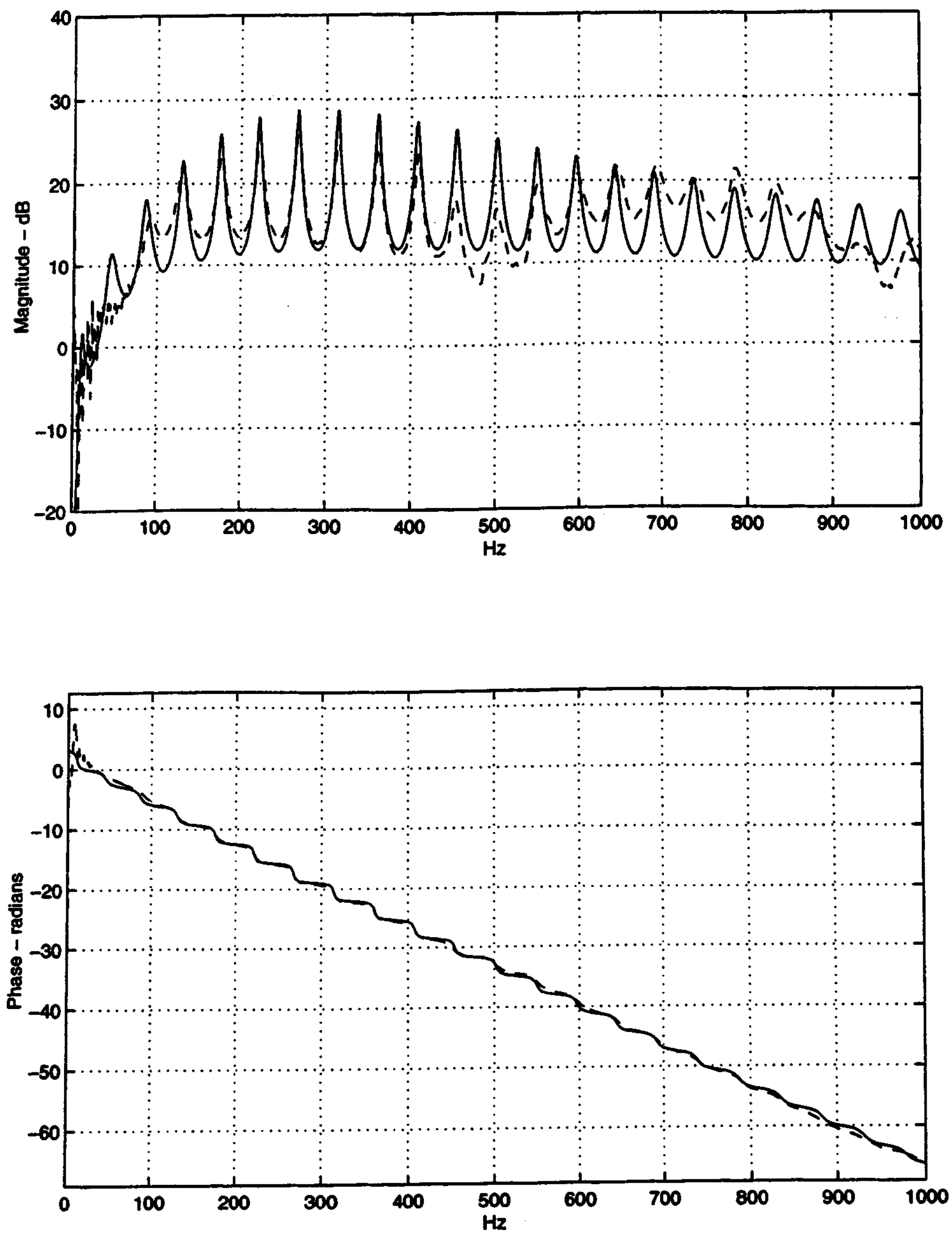

Fig. 6 Measured (dashed) and calculated (solid) disturbance speaker to end microphone frequency responses.

$$-Az=y.$$

Define z as follows

$$z_1=\rho_o\int_L^x \psi(s)ds-My_2,$$

$$z_2=\frac{1}{\rho_o c^2}\int_0^x \phi(s)ds-\frac{A_D}{\pi a^2}y_3,$$

$$z_3=C\left(\frac{1}{R_1}+\frac{1}{R_2}\right)^{-1}\left[y_1+\frac{M}{CR_2}y_2\right],$$

$$z_4=z_2(L)-\frac{1}{R_2}z_1(L)-\frac{1}{R_2}z_3,$$

$$z_5=\frac{m_D}{k_D}\left[y_4-\frac{A_D}{M_D}z_1(0)+\frac{d_D}{m_D}y_3\right],$$

$$z_6=-y_3.$$

It can easily be verified that $z\in D(A)$ and that

$$-Az=y.$$

This completes the proof.

Appendix B: Transfer Function Solution

Here we provide a brief derivation of the relevant transfer functions. Further details can be found in Refs. [18,19]. Consider the differential equation in variable x,

$$G_{\zeta\zeta}(\zeta,x)-k^2G(\zeta,x)=\delta(\zeta-x), \tag{29}$$

where $k=s/c$. Let G be the generalized solution to this second-order ordinary differential equation (ODE)

$$G(\zeta,x)=\begin{cases} Ae^{k\zeta}+Be^{-k\zeta} & 0\leq\zeta\leq x \\ Ce^{k\zeta}+De^{-k\zeta} & x\leq\zeta\leq L \end{cases}. \tag{30}$$

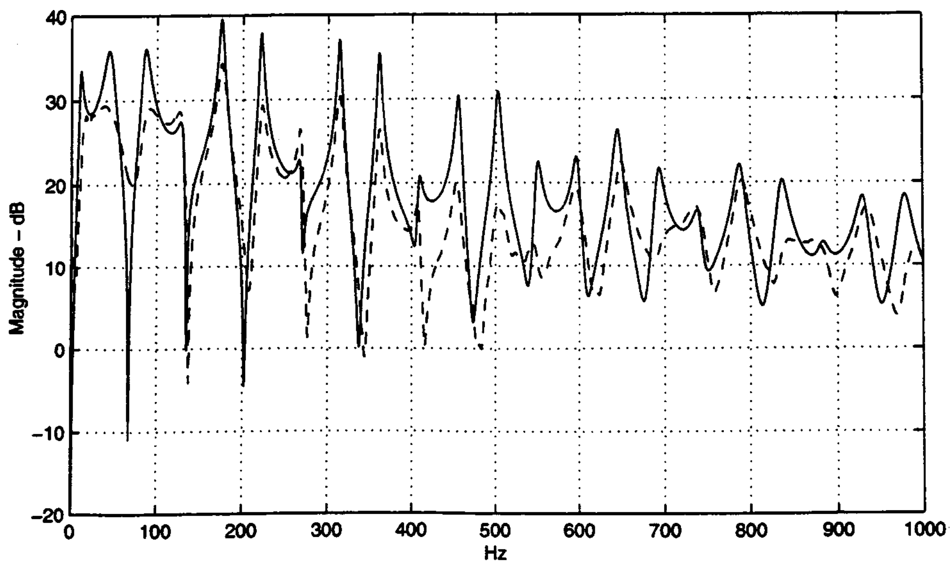

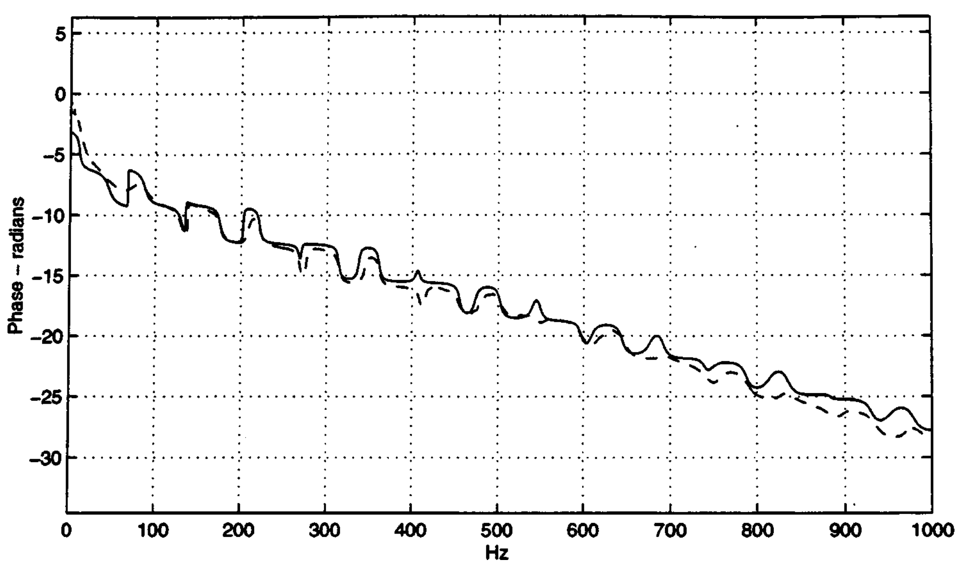

Fig. 7 Measured (dashed) and calculated (solid) disturbance speaker to mid microphone frequency responses.

The choice of coefficients A, B, C, D is made using the boundary conditions, so that pressure $p(x)$ can be calculated from $G(\zeta,x)$.

To this end, examine the integral

$$\int_0^L f(\zeta)G(\zeta,x)d\zeta=\int_0^L G(\zeta,x)(p_{\zeta\zeta}(\zeta)-k^2p(\zeta))d\zeta.$$

Integrating the right-hand side by parts, gives

$$G(L,x)p_x(L)-G_\zeta(L,x)p(L)-G(0,x)p_x(0)$$
$$+G_\zeta(0,x)p(0)+\int_0^L p(\zeta)[G_{\zeta\zeta}(\zeta,x)-k^2G(\zeta,x)]d\zeta.$$

Substituting the conditions in Eqs. (22) and (29) we obtain

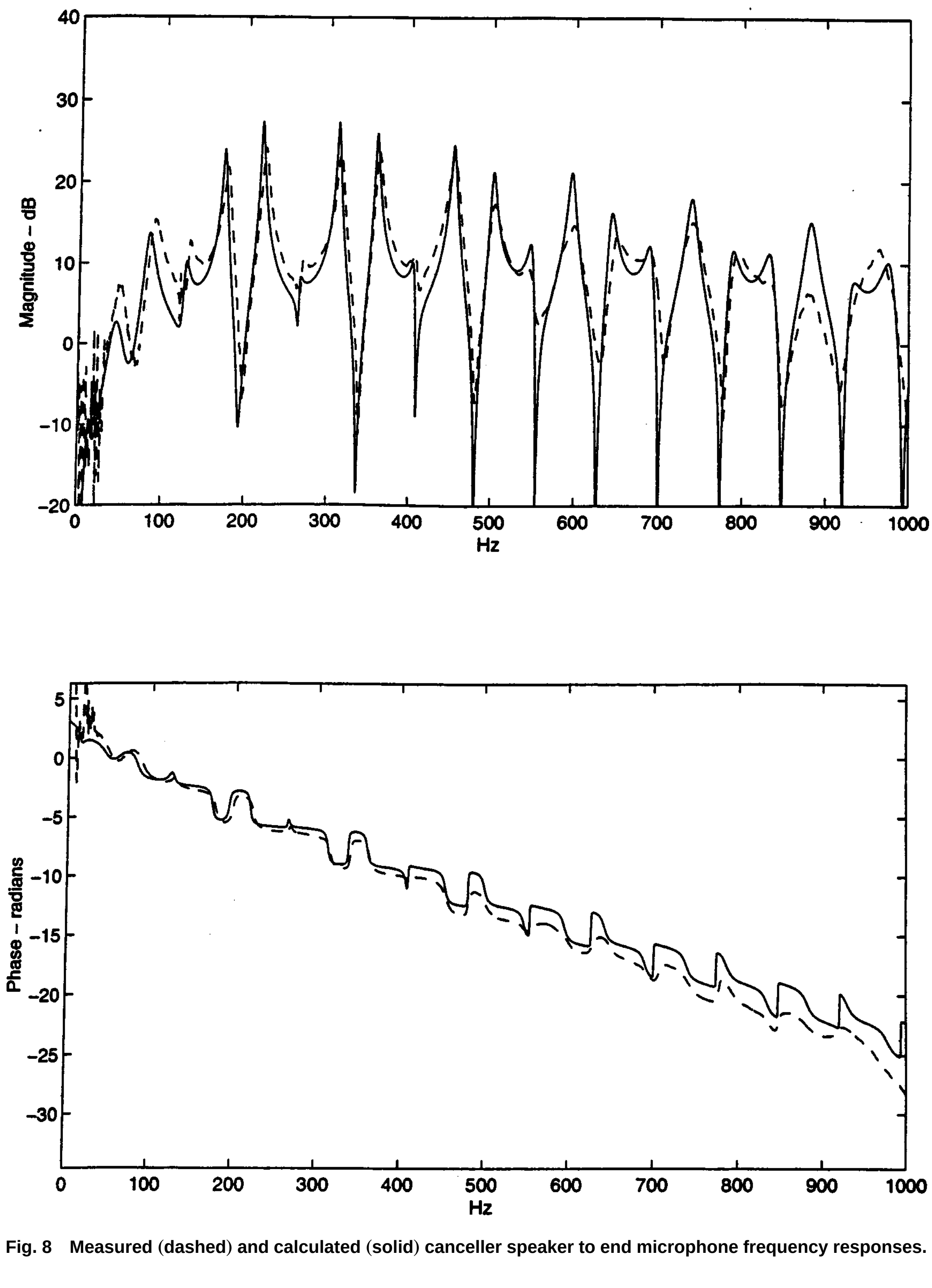

Fig. 8 Measured (dashed) and calculated (solid) canceller speaker to end microphone frequency responses.

$$\int_0^L f(\zeta)G(\zeta,x)d\zeta = \left[G(L,x)\left(\frac{-\rho_0 s}{Z_L(s)}\right) - G_\zeta(L,x)\right]p(L) + \left[G(0,x)\left(\frac{-A_D\rho_0 s}{Z_0(s)}\right) + G_\zeta(0,x)\right]p(0) + \frac{G(0,x)\rho_0 s}{Z_0(s)}g(s) + p(x), \quad (31)$$

where

$$Z_0 = \frac{\pi a^2}{A_D s}(m_D s^2 + d_D s + k_D),$$

$$Z_L = \pi a^2 \frac{(R_1+R_2)Ms + R_1R_2MCs^2}{(R_1+R_2)+(M+R_1R_2C)s+R_1MCs^2},$$

and $g(s) = \dfrac{Bl}{R_{coil}}E_D$.

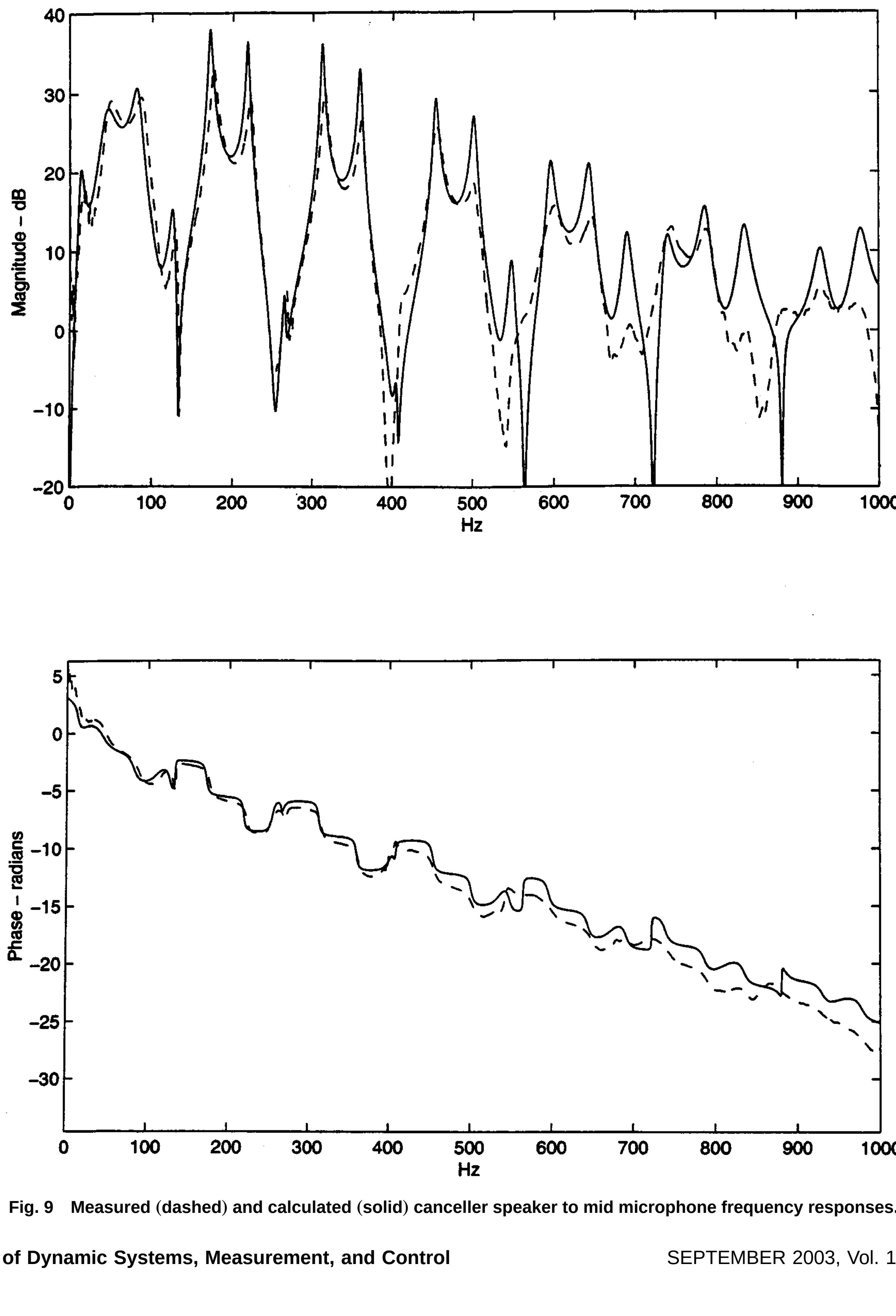

Fig. 9 Measured (dashed) and calculated (solid) canceller speaker to mid microphone frequency responses.

To eliminate the first two terms on the right-hand side of Eq. (31), we choose the following conditions on G

$$G(L,x)\frac{\rho_0 s}{Z_L(s)}+G_\zeta(L,x)=0, \tag{32}$$

$$G(0,x)\frac{\rho_0 s A_D}{Z_0(s)}-G_\zeta(0,x)=0. \tag{33}$$

Now, examine the equation

$$G_{\zeta\zeta}(\zeta,x)-k^2G(\zeta,x)=\delta(\zeta-x),$$

which when integrated from $\zeta=x_-$ to x_+ gives

$$G_\zeta(\zeta,x)\big|_{x_-}^{x_+}-k^2\int_{x_-}^{x_+}G(\zeta,x)d\zeta=1.$$

Since we assume that $G(\zeta,x)$ is continuous at $\zeta=x$, the second term on the left equals zero, and thus we have the condition

$$G_\zeta(\zeta,x)\big|_{x_-}^{x_+}=1. \tag{34}$$

Equations (33), (32), and (34) respectively imply that

$$-(A+B)\frac{\rho_0 s A_D}{Z_0(s)}+k(A-B)=0, \tag{35}$$

$$(Ce^{kL}+De^{-kL})\frac{\rho_0 s}{Z_L(s)}+k(Ce^{kL}-De^{-kL})=0, \tag{36}$$

$$Cke^{kx}-Dke^{-kx}-Ake^{kx}+Bke^{-kx}=1. \tag{37}$$

The continuity of $G(\zeta,x)$ at $\zeta=x$ implies

$$Ae^{kx}+Be^{-kx}=Ce^{kx}+De^{-kx}. \tag{38}$$

From Eqs. (35) and (36) we obtain that

$$B=\alpha_0 A,\quad \text{where}\quad \alpha_0=\frac{Z_0(s)-\rho_0 cA_D}{Z_0(s)+\rho_0 cA_D} \tag{39}$$

and

$$C=\alpha_L e^{-2Lk}D,\quad \text{where}\quad \alpha_L=\frac{Z_L(s)-\rho_0 c}{Z_L(s)+\rho_0 c}. \tag{40}$$

From Eqs. (37) and (38) it follows that

$$(C-A)=\frac{1}{2k}e^{-kx} \tag{41}$$

and

$$(B-D)=\frac{1}{2k}e^{kx}. \tag{42}$$

Combining the above equations, we solve for A, B, C, D to obtain

$$A=\frac{\alpha_L e^{-2Lk}e^{kx}+e^{-kx}}{2k(\alpha_0\alpha_L e^{-2Lk}-1)},$$

$$B=\frac{\alpha_0(\alpha_L e^{-2Lk}e^{kx}+e^{-kx})}{2k(\alpha_0\alpha_L e^{-2Lk}-1)},$$

$$C=\frac{\alpha_L e^{-2Lk}(e^{kx}+\alpha_0 e^{-kx})}{2k(\alpha_0\alpha_L e^{-2Lk}-1)},$$

$$D=\frac{e^{kx}+\alpha_0 e^{-kx}}{2k(\alpha_0\alpha_L e^{-2Lk}-1)}.$$

Thus

$$G(\zeta,x)=\frac{1}{2k(\alpha_0\alpha_L e^{-2Lk}-1)}\begin{cases}(\alpha_L e^{-2Lk}e^{kx}+e^{-kx})(e^{k\zeta}+\alpha_0 e^{-k\zeta}) & 0\leqslant\zeta\leqslant x\\ (\alpha_L e^{-2Lk}e^{k\zeta}+e^{-k\zeta})(e^{kx}+\alpha_0 e^{-kx}) & x\leqslant\zeta\leqslant L\end{cases}. \tag{43}$$

So, from Eq. (31),

$$p(x)=\frac{-G(0,x)\rho_0 s}{Z_0}g(s)+\int_0^L f(\zeta)G(\zeta,x)d\zeta. \tag{44}$$

From Eq. (44) it can be seen that the transfer function that relates the pressure measured at x to the voltage applied to the disturbance loudspeaker at $x=0$ is

$$\frac{p(x)|_{V_c=0}}{E_D(s)}=G_d(s,x,0),$$

$$\text{where}\quad G_d(s,x,0)=\frac{\rho_0 c}{Z_0}\frac{Bl}{R_{coil}}\frac{(1+\alpha_0)(\alpha_L e^{kx}+e^{-kx})}{2(1-\alpha_0\alpha_L)}.$$

Similarly, the transfer function that relates pressure measured at x to the total volume velocity V_c generated by the canceller loudspeaker at $x=x_c$ is

$$G_{cv}(s,x,x_c)=\frac{p(x)|_{g=0}}{V_c},$$

where, letting $\hat{V}$ indicate the Laplace transform of $V(x,t)$,

$$G_{cv}(s,x,x_c)V_c=\int_0^L\frac{-\rho_0 s}{\pi a^2}\hat{V}(\zeta,s)G(\zeta,x)d\zeta. \tag{45}$$

We now evaluate the integral (45). Substituting in the definition of $\hat{V}(\zeta,s)$, we obtain

$$G_{cv}(s,x,x_c)=\frac{-\rho_0 s}{\pi a^2\pi r_c^2}\int_{x_c-r_c}^{x_c+r_c}2\sqrt{r_c^2-(\zeta-x_c)^2}G(\zeta,x)d\zeta, \tag{46}$$

where G is as defined in Eq. (43). For $x_c+r_c\leqslant x$, substitute $G(\zeta,x)$ into Eq. (46) to obtain, writing $k=s/c$,

$$\frac{G_{cv}(s,x,x_c)}{V_c}=\frac{\rho_0 c}{\pi a^2\pi r_c^2}\frac{1}{2(1-\alpha_0\alpha_L e^{-2Lk})}\times(\alpha_L e^{-2Lk}e^{kx}+e^{-kx})\mathcal{I},$$

where

$$\mathcal{I}=\int_{x_c-r_c}^{x_c+r_c}2\sqrt{r_c^2-(\zeta-x_c)^2}(e^{k\zeta}+\alpha_0 e^{-k\zeta})d\zeta. \tag{47}$$

We need to calculate the integral $\mathcal{I}$. Using the change of variables

$$\zeta=x_c+r_c\cos\theta,\quad d\zeta=-r_c\sin\theta d\theta, \tag{48}$$

$$\mathcal{I}=2r_c^2e^{x_ck}\int_0^\pi e^{kr\cos\theta}\sin^2\theta d\theta+2r_c^2e^{-x_ck}\alpha_0\int_0^\pi e^{-kr\cos\theta}\sin^2\theta d\theta. \tag{49}$$

From a standard table of integrals

$$\int_0^{\pi} e^{ikq\cos\theta}\sin^2\theta d\theta=\frac{\pi}{kq}J(1,kq), \tag{50}$$

where $J(1,x)$ is the Bessel function of the first kind of order 1 evaluated at x. Thus,

$$\mathcal{I}=\pi r_c^2\left[e^{x_c k}2\frac{J(1,-ikr_c)}{-ikr_c}+\alpha_0 e^{-x_c k}2\frac{J(1,ikr_c)}{ikr_c}\right]. \tag{51}$$

Similarly, for $x\leqslant x_c-r_c$, we need to evaluate

$$\mathcal{I}=\int_{x_c-r_c}^{x_c+r_c}2\sqrt{r_c^2-(\zeta-x_c)^2}(e^{-k\zeta}+\alpha_L e^{-2Lk}e^{k\zeta})d\zeta.$$

Using the substitution (48), we obtain as above

$$\mathcal{I}=\pi r_c^2\left[\alpha_L e^{-2Lk}e^{x_c k}2\frac{J(1,-ikr_c)}{-ikr_c}+e^{-x_c k}2\frac{J(1,ikr_c)}{ikr_c}\right]. \tag{52}$$

Define $J(z)=2J(1,z)/z$. Substituting Eqs. (51) or (52) as appropriate into Eq. (46), we obtain that

$$G_{cv}(s,x_c)=\frac{\rho_0 c}{2\pi a^2(1-\alpha_0(s)\alpha_L(s)e^{-2L\,s/c})}\tilde{G}(s),$$

where

$$\tilde{G}(s)=\begin{cases}(\alpha_L(s)e^{(-2L+x)(s/c)}+e^{-(s/c)x})\left(e^{x_c(s/c)}J\left(-ir_c\frac{s}{c}\right)+\alpha_0(s)e^{-x_c(s/c)}J\left(ir_c\frac{s}{c}\right)\right) & 0<x_c\leqslant x\\ \left(\alpha_L(s)e^{(x_c-2L)(s/c)}J\left(-ir_c\frac{s}{c}\right)+e^{-(s/c)x_c}J\left(ir_c\frac{s}{c}\right)\right)\left(e^{x(s/c)}+\alpha_0(s)e^{-x(s/c)}\right) & x\leqslant x_c<L\end{cases}. \tag{53}$$

Using the loudspeaker model (21), we obtain the overall transfer function from canceller speaker voltage to acoustic pressure (26).

References

[1] Elliot, S. J., and Nelson, P. A., 1993, ''Active noise control,'' IEEE Signal Process. Mag., **10**, pp. 12–35.

[2] Seto, W. W. 1972, *Theory and Problems of Acoustics*, McGraw-Hill, Inc., New York.

[3] Hong, J., Akers, J. C., Venugopal, R., Lee, M.-N., Sparks, A. G., Washabaugh, P. D., and Bernstein, D. S., 1996, ''Modeling, identification, and feed-back control of noise in an acoustic duct,'' IEEE Trans. Control Syst. Technol., **4**, pp. 283–291.

[4] Hull, A. J., Radcliffe, C. J., and Southward, S. C., 1993, ''Global active noise control of a one-dimensional acoustic duct using a feedback controller,'' ASME J. Dyn. Syst., Meas., Control, **115**, pp. 488–494.

[5] Hull, A. J., and Radcliffe, C. J., 1991, ''An eigenvalue based acoustic impedance measurement technique,'' ASME J. Vibr. Acoust., **113**, pp. 250–254.

[6] Hull, A. J., Radcliffe, C. J., and MacCluer, C. R., 1991, ''State estimation of the nonself-adjoint acoustic duct system,'' ASME J. Dyn. Syst., Meas., Control, **113**, pp. 122–126.

[7] Morris, K. A., 1998, ''Noise reduction in ducts achievable by point control,'' ASME J. Dyn. Syst., Meas., Control, **120**, pp. 216–223.

[8] Spiekermann, C. E., and Radcliffe, C. J., 1988, ''Decomposing one-dimensional acoustic pressure response into propagating and standing waves,'' J. Acoust. Soc. Am., **84**(4), pp. 1536–1541.

[9] Levine, H., and Schwinger, J., 1948, ''On the radiation of sound from an unflanged circular pipe,'' Phys. Rev., **73**, pp. 383–406.

[10] Hu, J. S., 1995, ''Active sound attenuation in finite-length ducts using close-form transfer function models,'' ASME J. Dyn. Syst., Meas., Control, **117**, pp. 143–154.

[11] Birdsong, C., and Radcliffe, C. R., 1999, ''A compensated acoustic actuator for systems with strong dynamic pressure coupling,'' ASME J. Vibr. Acoust., **121**, pp. 89–94.

[12] Lane, S. A., and Clark, R. L., 1998, ''Improving loudspeaker performance for active noise control applications,'' J. Audio Eng. Soc., **46**, pp. 508–518.

[13] Morse, P. M., and Feshbach, H. 1953, *Methods of Theoretical Physics*, McGraw-Hill, Inc., New York.

[14] Beranek, L. L., 1986, *Acoustics*, American Institute of Physics, Inc., New York.

[15] Pierce, A. D. 1981, *Acoustics: An Introduction to Its Physical Principles and Applications*, McGraw-Hill, New York.

[16] Morse, P. M., and Ingard, K. N., 1986, *Theoretical Acoustics*, Princeton University Press.

[17] Pazy, A. 1983, *Semigroups of Linear Operators and Applications to Partial Differential Equations*, Springer-Verlag, New York.

[18] Obasi, E. E., 2002, *An Improved One-Dimensional Duct Model and Robust H_∞ Controller Design for Active Noise Control*, M. Math. Thesis, University of Waterloo.

[19] Zimmer, B. 1999, *An Improved One-Dimensional Model for Active Noise Control*, M. Math. Thesis, University of Waterloo.